

Study of $C_3H_5^+$ ion deposition on polystyrene and polyethylene surfaces using molecular dynamics simulations

Inkook Jang, Roshenda Phillips, and Susan B. Sinnott^{a)}

Department of Materials Science and Engineering, University of Florida, Gainesville, Florida 32611-6400

(Received 1 April 2002; accepted for publication 25 June 2002)

Molecular dynamics simulations of ion deposition processes are used to study the deposition of $C_3H_5^+$ ions on crystalline polystyrene (PS) and polyethylene (PE) surfaces at energies of 50 and 25 eV. For each system, 80 trajectories are carried out on pristine surfaces and the incident angle in every case is normal to the surface. The forces are determined using the reactive empirical bond order method developed by Tersoff and parametrized for hydrocarbons by Brenner, coupled to long-range Lennard–Jones potentials. The simulations predict that the ions deposited at 50 eV either dissociate and stick to the surface or remain on the surface intact in 98% of the trajectories on PS, and in 89% of the trajectories on PE. At 25 eV, the ions are deposited intact in 70% of the trajectories on PS and dissociate in only 3%. No dissociation of the incident ions is predicted to occur on PE at 25 eV. Rather, the ions scatter away in 90% of the trajectories. Consequently, ion deposition on PE at 25 eV is predicted to be very inefficient for thin-film growth. Many more ions or major ion fragments (such as C_2H_n and CH_2) remain near the surface on PS than PE at 50 eV. Thus, in general, polyatomic ion deposition for thin film growth is more efficient on PS than PE, and deposition at 50 eV is more efficient than deposition at 25 eV. © 2002 American Institute of Physics. [DOI: 10.1063/1.1500788]

I. INTRODUCTION

Computer simulations of the deposition of ions of specific mass and kinetic energy have been used to better understand the complex mechanisms associated with the processes used to grow polymer thin films in plasmas.^{1,2} Even though plasma treatments are widely used to improve surface properties and deposit surface coatings, the detailed mechanisms of interaction between reactants in the plasma and the surface are difficult to determine experimentally. Computer simulation is one method that can be used to specify reaction conditions, such as surface structure, and isolate the effect of individual species. Therefore, computer simulation is a useful tool for the study of possible interaction mechanisms between reactant species and the surface under specific reaction conditions.^{1,3,4}

Low energy plasma surface treatments can be used to graft specific functional groups or grow polymeric films on surfaces. For example, fluorocarbon plasma deposition has been used to grow fluorinated polymer films on various surfaces to yield films with high thermal and chemical resistance, high dielectric constants, and low friction coefficients.^{5,6} Hydrocarbon plasma deposition has also been widely used to yield thin films with high hardness and specific electronic band-gap characteristics.^{7–9} For instance, these plasma processes have been used to produce protective coatings, improve the adhesive strength of films with polymer materials, tailor the surface properties of biomedical, electronic, and optical devices, and produce mem-

branes for specific purposes such as fuel cells and gas separation.^{2,5–8,10–12}

In previous work, we examined the deposition of CH_3^+ and $C_3H_5^+$ on crystalline polystyrene (PS) surfaces at kinetic energies of 20–100 eV using molecular dynamics (MD) simulations and compared the results to experimental findings for the analogous fluorocarbon ions CF_3^+ and $C_3F_5^+$ on PS.^{1,3} The experiments and simulations showed that $C_3F_5^+/C_3H_5^+$ ions were more effective at growing films than the CF_3^+/CH_3^+ ions when they were deposited at similar energies per atom (~ 6 eV/atom). Fragmentation of both types of ions increased when the ion energies were increased in both the experiments and simulations. We also investigated the effect of changing the incident angle of the $C_3H_5^+$ ions during deposition on the PS surface using MD simulations at fixed incident energies of 50 eV.¹³ These simulations predicted that small inclined angles, such as 45° from the surface normal, were more efficient for the deposition of the precursors necessary to form thin polymer films, even though the total amount of deposited carbon that remained on the surface was largest at normal incidence. This was because more ions or ion fragments remained near the surface at 45° than at 0° . In addition, the number of CH_2 fragments that remained at the surface was largest at 45° . This is significant because CH_2 was predicted to be the most reactive species in our simulation; the majority of these fragments bonded to the PS backbones.

The surface reactions that incident ions undergo are expected to be different on different surfaces. The chemical and physical properties of the surface are expected to affect the interaction between incident ions (or their fragments) and the surface. In this article, we compare $C_2H_5^+$ deposition on

^{a)} Author to whom correspondence should be addressed; electronic mail: ssinn@mse.ufl.edu

crystalline PS and polyethylene (PE) surfaces at 50 and 25 eV and normal incidence using classical MD simulations. These surfaces were selected because PE and PS are composed of the same elements, carbon and hydrogen, but have very different chemical and physical properties. For example, PS has a higher glass transition temperature and melting temperature, and a stiffer structure than PE. These differences come from the presence of the bulky phenyl ring in the PS structure.¹⁴ Thus, this study will provide insight into the atomic-scale effects of surface chemical and physical structures on reaction mechanisms.

II. COMPUTATIONAL DETAILS

The MD simulations numerically integrate Newton's equations of motion with a third-order Nordsieck predictor corrector¹⁵ using a time step of 0.2 fs. Short-range interatomic forces are calculated using the reactive empirical bond order potential developed by Tersoff,^{16,17} and parameterized by Brenner for hydrocarbons,¹⁸ and refined within the last few years.¹⁹ Unlike molecular mechanics models, this potential can predict new bond formation and bond breaking which are important processes in polyatomic ion deposition and surface modification. It has been successfully used to obtain insight into various processes such as molecule-surface collisions,²⁰ cluster-surface deposition,^{21,22} and the chemical vapor deposition of diamond.^{23,24} Long-range van der Waals interactions are included in the form of a Lennard-Jones potential that is only active at distances greater than the covalent bond lengths.¹⁵

Because of the empirical, classical nature of these potentials, electronic effects such as electronic excitations or charging of the atoms are not included. Therefore, ions with positive charges are treated as reactive radicals rather than true ions with an actual charge. It is recognized that the presence of a positive charge will influence the chemical reactions that occur during deposition. However, it is also true that many incident ions are rapidly neutralized as they approach the surface. The expectation is that the simulation results are qualitatively correct and can provide insight into the processes taking place during polyatomic ion deposition on PS and PE.

The PS and PE surfaces used in the simulations contain eight and ten layers, respectively, for a total thickness of 50 Å. The bottom layer of the surface and atoms within 2.5 Å from the four sides of the slab have Langevin frictional forces applied to maintain the surface temperature at 300 K.¹⁵ This imitates the heat dissipation process of real surfaces. The rest of the atoms in the system have no constraints and are designated as active. Periodic boundary conditions are also applied within the plane of the surface to mimic an infinite surface and effectively double the number of thermostat atoms at the edges of the surface.

The simulations are performed with the ground state isomeric structure of $C_3H_5^+$ ($CH_2-C^+H-CH_2$). It was previously predicted that the ground state structure is most prevalent experimentally, despite the fact the ions have significant internal energy that could lead to excited isomeric structures.¹ The ions are deposited at various locations within

TABLE I. Percentage of occurrence of the indicated events in the MD simulations of $C_3H_5^+$ deposition averaged over 80 trajectories.

	PS		PE	
	50eV	25eV	50eV	25eV
Simple scattering from the surface	2.2	27.5	7.5	77.5
Scattering from the surface with a captured surface hydrogen			3.8	12.5
Embedding within the surface	22.5	51.3	6.3	3.8
Incorporation with the surface	15.7	18.8	42.5	6.3
Dissociation (losing one or more H atoms)	27.9	1.3	13.8	
Dissociation $CH_2+C_2H_3$	23.6	1.3	17.5	
Dissociation $CH_3+C_2H_2$	1.1		3.8	
Dissociation $CH_2+C_2H_2+H$	4.5		3.8	
Dissociation $CH+C_2H_3+H$	3.4			
Dissociation $CH+CH_2+CH_2$			1.3	

the active region of the surface at several orientations relative to the surface. The total kinetic energies of the ions are 25 and 50 eV and the incident angle is normal to surface. Deposition at each condition is examined in 80 trajectories and the simulations run from 0.2 to 1.2 ps before it is determined that the results have reached a steady state.

III. RESULTS AND DISCUSSION

Table I summarizes the results obtained from the MD simulations for PS and PE surfaces at ion energies of 50 and 25 eV. The ion fragments indicated in the table react with the surface atoms after dissociation in most cases. Therefore, the exact structures of the fragments may be different from the structures shown in the table after equilibration has occurred. No carbon atoms are removed from the polymer surfaces. However, some hydrogen atoms are detached from the polymer chains and knocked loose from the surface. Therefore, etching effects are predicted to be negligible in all the cases considered.

Ions dissociate on the PS surface in many more trajectories than on the PE surface at 50 eV. On the PS surfaces, 61% of the incident ions dissociate in the trajectories, whereas they dissociate in 40% of the trajectories on the PE surfaces. On both PS and PE surfaces, the loss of hydrogen atom(s) and the $C_2H_5 \rightarrow CH_2 + C_2H_3$ dissociation reaction are the most common chemical reactions. At 25 eV, only a few ions dissociate on the PS surfaces and the ions deposit intact in 70% of the trajectories. No ion dissociates on the PE surfaces at 25 eV and the ions remain on the surface in only 10% trajectories. Small fragments of ions or radicals generated in fluorocarbon plasma, such as CF_2 , are considered to be important precursors to polymer film formation.²⁵⁻²⁸ Therefore, it can be inferred that ion energies of 25 eV are a poor choice for thin film formation on PS because most of the incident ions remain intact.

The PS is stiffer than the PE because molecular motions are hindered by the bulky phenyl rings. When the incident ions hit the PS chains, the impact energy cannot be absorbed through deformation of the chains as efficiently as is the case in PE. Therefore, the impact energy is concentrated on a smaller part of the PS chains and leads to the dissociation of

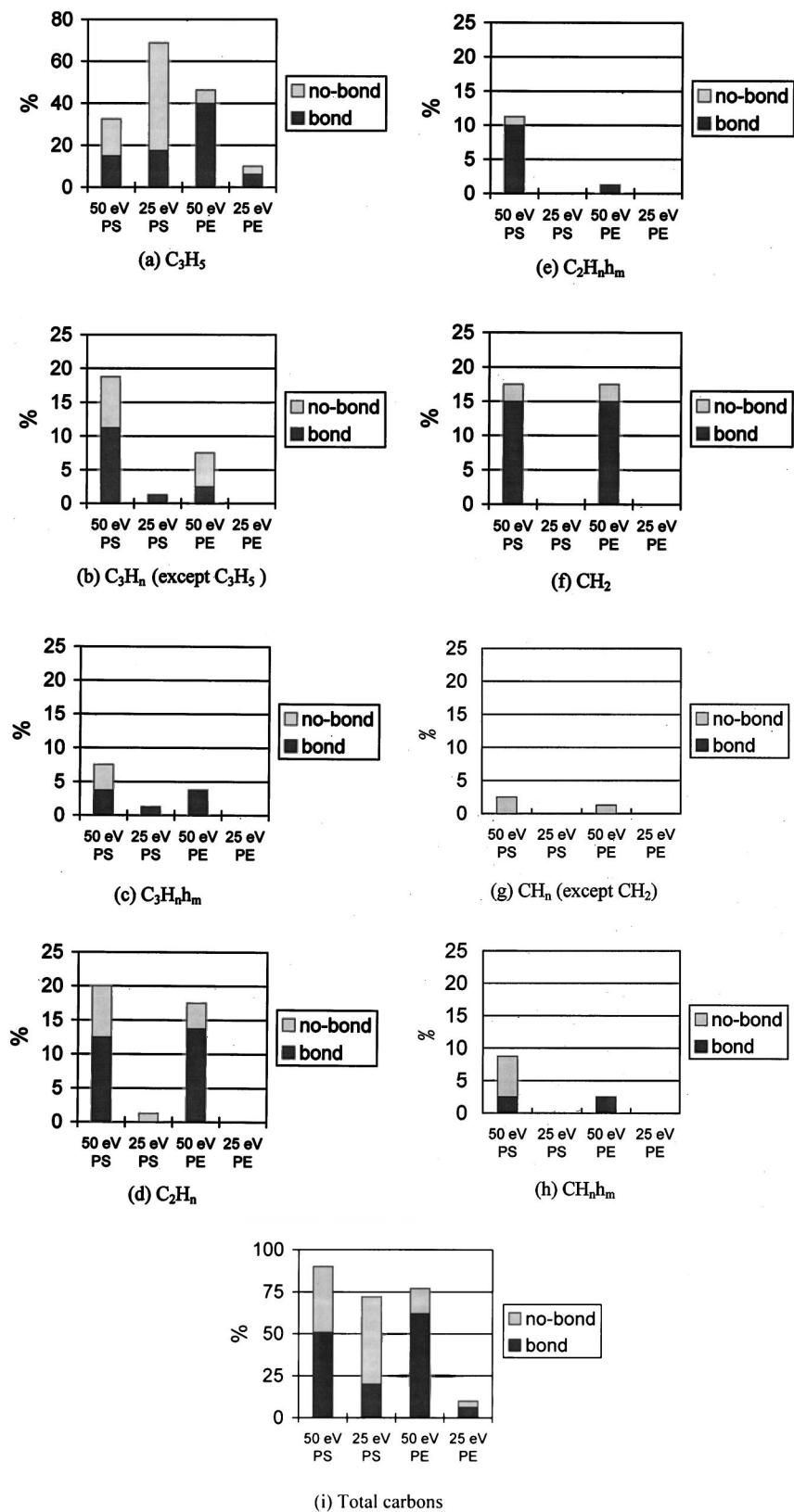


FIG. 1. Percentages of the indicated product species that remain bonded to carbon atoms in, or are embedded within, the PS and PE surfaces at 50 and 25 eV. The results represent the averaged data from 80 MD simulation trajectories. "Bond" means that the indicated species formed bonds with carbon atoms in the polymer substrates on the time scales of the simulations. "No-bond" means that the indicated species were embedded in the polymer substrate but did not form covalent bonds with carbon atoms in the polymer on the time scales of the simulations.

the incident ions more easily than on PE. This result agrees with the findings of other reports in the literature.^{21,29,30}

Ions scatter from the surface in many more trajectories on the PE surface than on the PS surface. At 25 eV, the ions are scattered away in 90% of the trajectories on the PE surface, whereas ions scatter from the PS surface in only 28% of

the trajectories. As mentioned above, the PE chains can accommodate the impact energy by deformation through several chain segments. The excess energy can then be dissipated through the whole surface in the form of heat, which is removed through the Langevin frictional forces in the heat bath atoms. The energy can also be removed by restoring

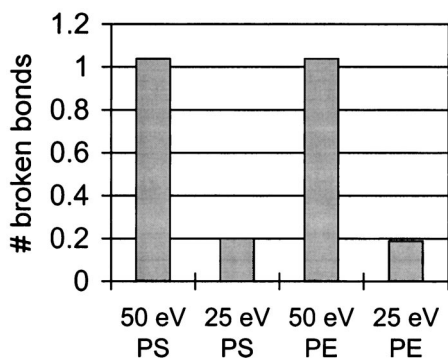


FIG. 2. Average number of broken bonds in the PS and PE surfaces per MD trajectory as a result of $C_3H_5^+$ deposition at 50 and 25 eV. The results are averaged over 80 trajectories.

deformed chains to their original conformation that causes the incident ions to scatter from the surface. This mechanism is not favorable for PS due to the lack of chain mobility. At 50 eV, ions scatter from the surfaces in only 2% of the trajectories on PS and 11% of the trajectories on PE. Some ions abstract hydrogen atoms from the surface as they scatter away, especially on the PE surface. On the PS surface, if the incident ions detach hydrogen atoms from the surface carbon atoms, they do not escape from the surface without dissociation.

Figure 1 summarizes the number of ion fragments that are bonded to, or embedded in, the PS and PE surface at 50 and 25 eV 0.8–1.2 ps after deposition. The embedded fragments penetrate the polymer surfaces but do not form covalent bonds with the carbon atoms of the polymers on the time scale of these simulations. Following the notation used in our previous paper, “C” and “H” represent carbon and hydrogen from the incident ion while “h” is hydrogen from the polymer surfaces.^{1,13} Overall, more fragments remain on the PS surface than on the PE surface. The exception is C_3H_5 ions, more of which remain on the PE surface than the PS surface at 50 eV. This is because more incident ions dissociate on the PS surface than on the PE surface [see Fig. 1(a)].

Figure 1(b) shows that many more C_3H_n fragments, generated from incident ions that lose one or some hydrogen atoms, are deposited on the PS surface than on the PE surface. At 25 eV, there is no ion fragmentation on the PE surface and only a few incident ions remain intact. This is be-

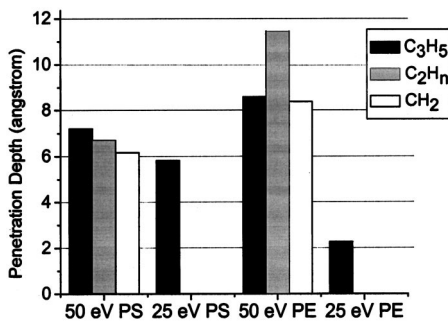


FIG. 3. Averaged penetration depths of major species (C_3H_5 , C_2H_n , CH_2) from the incident ions.

cause most of the ions scatter from the surface without dissociation. In contrast, 70% of incident ions remain on the PS surface, but the majority of them are merely embedded in the surface because 25 eV is not enough energy for the formation of new bonds with the surface atoms on the time scales of these simulations.

For the major fragments, C_2H_n and CH_2 , similar amounts are deposited on both surfaces as shown in Figs. 1(d) and 1(f). Slightly more C_2H_n stay on the PS surface, but the amount of CH_2 is almost the same on both surfaces. In previous work, we predicted that the CH_2 fragments play an important role in the cross linking of the PS surface.¹³ Excluding CH_2 , only a small number of fragments that contain one carbon atom remain on either surface at 50 eV [Fig. 1(g)].

The fragments that recombine with surface hydrogen atoms, $C_3H_nh_m$, $C_2H_nh_m$, and CH_nh_m , are more readily found on the PS surface than the PE surface [Figs. 1(c), 1(e), and 1(h)]. This means that more hydrogen atoms are abstracted from polymer chains on the PS surface than on the PE surface. Figure 2 shows the average number of carbon–hydrogen and carbon–carbon bonds that are broken in the polymer as a result of the ion deposition. The number of broken bonds is almost the same for both polymers. As mentioned earlier, PE is more effective at dissipating the energy of impact than PS due to the increased flexibility of its chains. One might therefore infer that bonds in the PS surface may be broken more easily than bonds in the PE surface. However, 67% of carbon–carbon bonds in the PS surface are in phenyl rings. The energy needed to break carbon–carbon bonds in the phenyl rings is greater than that needed to break single carbon–carbon bonds, such as are found on the PE surface. Specifically, the calculated bond energy of a single carbon–carbon bond is 3.69 eV while the calculated bond energy of a conjugated double carbon–carbon bond is 5.36 eV according to the reactive empirical bond-order potential used in the simulations.¹⁹ Therefore, the probability of carbon–carbon bond dissociation in the PS is lower than that in the PE if the same energy is applied per carbon–carbon bond. This property compensates for the effectiveness of the PE in absorbing the impact energy, and makes the numbers of broken bonds almost the same for both polymers. The partial saturation of the phenyl rings on the PS occurs infrequently in the simulations. The vast majority of the interactions of the ions or ion fragments with the phenyl rings result in broken rings or the substitution of the ion or fragment for the phenyl hydrogen atoms. This is consistent with known aromatic chemistry³¹ that shows that partially saturated phenyl rings are unstable and usually go back to a resonance structure spontaneously by removing a hydrogen atom or substituent species.

The number of carbon–hydrogen bonds broken should be larger in PS than PE because the probability of carbon–carbon bond dissociation in PS is less for the same total number of broken bonds. This explains why more hydrogen atoms are detached from the PS surface than the PE surface.

Figure 1(i) summarizes the total amount of carbon deposited on the PS and PE surfaces averaged over the 80 trajectories at 50 and 25 eV. The amount of carbon deposited

on the PS surface is larger than on the PE surface, but the number of carbon atoms from the incident ions forming bonds with surface carbon atoms is larger on the PE surface at energies of 50 eV. When one carbon-carbon bond is broken, two reactive sites are formed in the polymer chain, whereas only one reactive site is made after breaking one carbon-hydrogen bond. Since carbon-carbon bond dissociation is more favorable on PE than PS, incident ions or fragments can form bonds with surface carbon atoms more easily on the PE surface. At 25 eV, most of the carbon deposited on the PS surface is in the form of intact incident ions, and only a small amount of carbon remains on the PE surface because most of the incident ions are scattered away.

Figure 3 shows the average penetration depth for the ions or significant ion fragments in PS and PE at 50 and 25 eV. The figure indicates that all three species penetrate more deeply into the PE surface than the PS surface at 50 eV. PE has better chain mobility than PS so that ions or fragments can squeeze into the PE substrate more easily. At 25 eV, the average penetration depth of the ions is smaller in PE than PS. However, the number of ions remaining on the PE surface is very small (10%) compared with the number of ions on the PS surface (70%). Therefore, the number of ions near the surface cannot be larger in PE than in PS.

IV. CONCLUSIONS

This computational study shows that the $C_3H_5^+$ ion deposition process to produce precursors for thin-film growth is more effective on the PS surface than on the PE surface, and deposition at 50 eV is more effective than deposition at 25 eV. More ions dissociate and remain on the PS surface, and more ions and fragments remain in a shallow region of the PS surface. In particular, at 25 eV the ion deposition process on the PE surface is very inefficient because 90% of the incident ions scatter from the surface. However, the amount of total carbon deposited on the PE surface is not much smaller than the amount deposited on the PS surface. The amount of major fragments (C_2H_n and CH_2) deposited on both surfaces at 50 eV is almost the same.

A minor property of the PE substrate expected from our results is that relatively more carbon-carbon bonds are broken by ion deposition on the PE surface than on the PS surface. This bond breaking can affect the mechanical strength of the substrate. However, it can also lead to the formation of reactive sites to which incident ions or ion fragments can attach.

Thus, the simulations illustrate the atomic-scale mechanisms responsible for the differing surface modification effects of $C_3H_5^+$ deposition on crystalline PS and PE surfaces. These mechanisms would be expected to be found in mass-

selected ion-beam deposition of polymer surfaces and in surface modification in plasma.

ACKNOWLEDGMENT

The authors gratefully acknowledge the support of the Petroleum Research Fund, administered by the American Chemical Society.

- ¹M. B. J. Wijesundara, Y. Ji, B. Ni, S. B. Sinnott, and L. Hanley, *J. Appl. Phys.* **88**, 5004 (2000).
- ²C. F. Abrams and D. B. Graves, *J. Vac. Sci. Technol. A* **19**, 175 (2001).
- ³M. B. J. Wijesundara, L. Hanley, B. R. Ni, and S. B. Sinnott, *Proc. Natl. Acad. Sci. U.S.A.* **97**, 23 (2000).
- ⁴C. F. Abrams and D. B. Graves, *J. Appl. Phys.* **86**, 5938 (1999).
- ⁵K. Tanaka, T. Inomata, and M. Kogoma, *Thin Solid Films* **386**, 217 (2001).
- ⁶M. E. H. M. da Costa, J. Freire, F. L., L. G. Jacobsohn, D. Franceschini, G. Mariotto, and I. R. J. Baumvol, *Diamond Relat. Mater.* **10**, 910 (2001).
- ⁷A. von Keudell, *Thin Solid Films* **402**, 1 (2002).
- ⁸R. U. A. Khan, J. V. Anguita, and S. R. P. Silva, *J. Non-Cryst. Solids* **276**, 201 (2000).
- ⁹A. Grill, *Diamond Relat. Mater.* **8**, 428 (1999).
- ¹⁰E. T. Ada, O. Kornienko, and L. Hanley, *J. Phys. Chem. B* **102**, 3959 (1998).
- ¹¹J. Feichtinger, R. Galm, M. Walker, K.-M. Baumgartner, A. Schulz, E. Rauchle, and U. Schumacher, *Surf. Coat. Technol.* **142-144**, 181 (2001).
- ¹²E. Finot, S. Roualdes, M. Kirchner, V. Rouessac, R. Berjoan, J. Durand, J.-P. Goudonnet, and L. Cot, *Appl. Surf. Sci.* **187**, 326 (2002).
- ¹³I. Jang, B. Ni, and S. B. Sinnott, *J. Vac. Sci. Technol. A* **20**, 564 (2002).
- ¹⁴L. H. Sperling, *Introduction to Physical Polymer Science*, 2nd ed. (Wiley, New York, 1992).
- ¹⁵M. P. Allen and D. J. Tildesley, *Computer Simulation of Liquids* (Oxford University Press, New York, 1987).
- ¹⁶J. Tersoff, *Phys. Rev. B* **37**, 6991 (1988).
- ¹⁷J. Tersoff, *Phys. Rev. B* **39**, 5566 (1989).
- ¹⁸D. W. Brenner, *Phys. Rev. B* **42**, 9458 (1990).
- ¹⁹D. W. Brenner, O. A. Shenderova, J. A. Harrison, S. J. Stuart, B. Ni, and S. B. Sinnott, *J. Phys.: Condens. Matter* **14**, 783 (2002).
- ²⁰E. R. Williams, G. C. Jones, L. Fang, R. N. Zare, B. J. Garrison, and D. W. Brenner, *J. Am. Chem. Soc.* **114**, 3207 (1992).
- ²¹L. F. Qi and S. B. Sinnott, *J. Vac. Sci. Technol. A* **16**, 1293 (1998).
- ²²L. F. Qi and S. B. Sinnott, *Nucl. Instrum. Methods Phys. Res. B* **140**, 39 (1998).
- ²³D. R. Alfonso, S. E. Ulloa, and D. W. Brenner, *Phys. Rev. B* **49**, 4948 (1994).
- ²⁴D. R. Alfonso and S. E. Ulloa, *Phys. Rev. B* **48**, 12235 (1993).
- ²⁵N. M. Mackie, V. A. Venturo, and E. R. Fisher, *J. Phys. Chem. B* **101**, 9425 (1997).
- ²⁶M. Inayoshi, M. Ito, M. Hori, T. Goto, and M. Hiramatsu, *J. Vac. Sci. Technol. A* **16**, 233 (1998).
- ²⁷D. C. Gray, V. Mohindra, and H. H. Sawin, *J. Vac. Sci. Technol. A* **12**, 354 (1994).
- ²⁸D. C. Gray, H. H. Sawin, and J. W. Butterbaugh, *J. Vac. Sci. Technol. A* **9**, 779 (1991).
- ²⁹L. Hanley, H. Lim, D. G. Schultz, S. B. Wainhaus, P. deSainte Claire, and W. L. Hase, *Nucl. Instrum. Methods Phys. Res. B* **125**, 218 (1997).
- ³⁰D. G. Schultz, S. B. Wainhaus, L. Hanley, P. deSainte Claire, and W. L. Hase, *J. Chem. Phys.* **106**, 10337 (1997).
- ³¹R. J. Fessenden and J. S. Fessenden, *Organic Chemistry*, 4th ed. (Brooks/Cole, Pacific Grove, CA, 1990).